POLITECNICO
MILANO 1863

SCUOLA DI INGEGNERIA INDUSTRIALE
E DELL'INFORMAZIONE

HOVENRING BRIDGE: ASSESSMENT OF THE TENSION IN STAY CABLES THROUGH AN EXPERIMENTAL CAMPAIGN

Department of Mechanical Engineering
Course of Dynamics of Mechanical Systems

Elisa Rita Rosanò 991950
Erika De Bardi 987096

Professor:
Prof. Alberto Zasso
Ing. Giulia Pomaranzi

Academic year:
2023-2024

Abstract: The aim of this assignment is the assessment of the tension of stay cables of a real system through an experimental campaign. This will lead to the final validation of the Finite Element (FE) model of the Hovenring bridge used for the analysis. From the results of free decay tests on 4 cables, the first natural frequencies (f_1) and associated non dimensional damping ratios (h_1) are derived. The cable tension in the FE model is varied until the experimental and numerical natural frequencies match. Finally, a comparison between the assessed tension values and the nominal design values for the considered cables can be carried out.

1. System description

Dealing with a suspended structures, bridges are designed to sustain the load exerted during their service life.

Figure 1: Hovenring bridge

Specifically, for the Hovenring bridge, we have a deck that allows the service ability of the structure; it is suspended by a tower that borne the load and it is able to transfer the weights thanks to stay cables from the deck to the ground, or from the constraint to the ground.

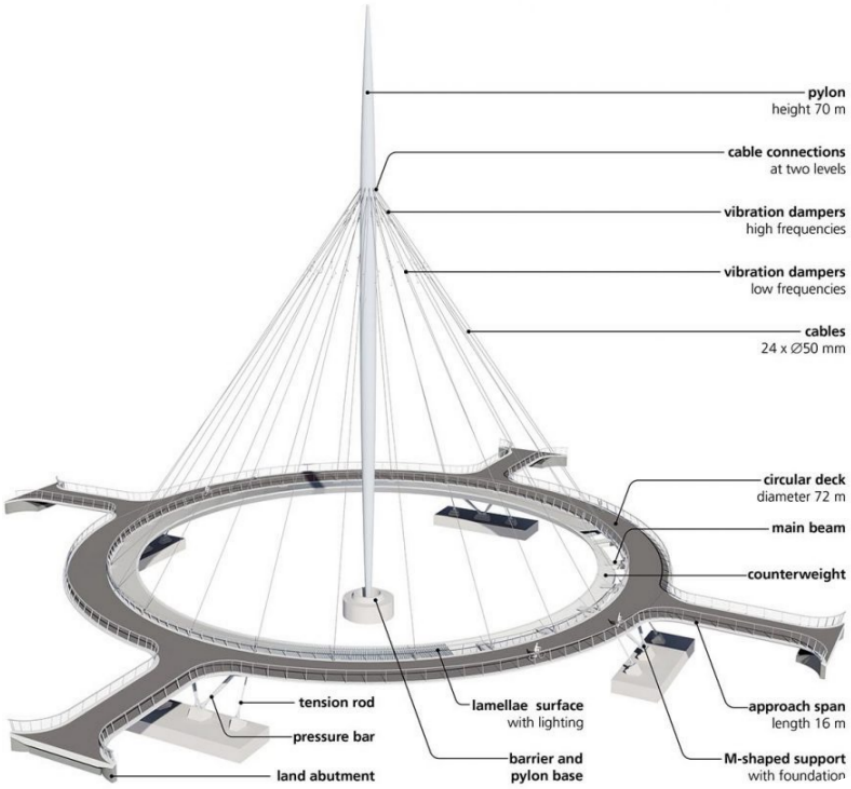

Figure 2: Hovenring bridge scheme

A central pylon 70m high is present, here 24 cables are connected at two different levels providing a different nominal length for the cables. It is important to notice that cables, placed over the lateral abutment, will express higher nominal tension because they are in correspondence of the constraints of the bridge to the ground. Thus, 4 different types of cables are present. Moreover, each cable has 2 different Tuned Mass Damper (TMD) that are effective in 2 frequency range: higher and lower frequencies.

During the designing phase of the bridge, tension forces are assigned to the cables allowing its support. Throughout the structure life, those theoretical values of tension forces can change or there can be a distribution of forces within the stays that no more reflect the values chosen in the designing process. Being an hyper-static structure, it is more difficult to understand how the forces and weights are redistributed, being easier just to compute the total loads. Thus, it is important to understand the actual tension force the stays have, before scheduling a re-tensioning of the cables; this is needed in order to execute a proper maintenance of the bridge.

2. Procedure description and objectives

An FE model replicating the dynamics of 4 cables has been developed for the present analysis. Consequently, the direct measurement of the cable tension thanks to a jacking system (dynamometer), combined with the first eigenfrequency f_1 detection through free motion tests, lead to the FE cable model validation. Once done, the tension of the 20 remaining cables is then estimated using the validated FE model and the experimental results.

This is possible since the first natural frequency is dependent on the tension force. The crucial step consists in changing the input tension force in the FE model, until the estimation of f_1 from the numerical model is the same as the one obtained experimentally. It is important to notice that only 4 cables out of 24 are interested by the direct measurement of the force through the jacking system since this procedure is extremely expensive.

For each cable is conducted an experimental campaign that will allow the estimation of the first eigenfrequency. Thus, free motion tests have been performed and 4 out of 24 are the total cable measurements under analysis for the method validation, in particular they are: $Cable5$, $Cable6$, $Cable8$ and $Cable13$. As a matter of fact, dealing with a cable, that is a continuous system (infinite number of natural frequencies), if it is excited within one of the resonance frequencies, the system response will be driven by that $\omega_{natural}$. Therefore, each cable is excited in the neighbor of the 1° natural frequency, so that from its experimental decay we can estimate the first eigenfrequency. Since this comes from measurements, it is representative of the actual loading condition of the system.

The operator is in charge of exciting by hand the cables according to an estimation of the first frequency that passes through the analytical model of the **pinned pinned cable**; then once the steady condition of the vibration mode is reached, each cable is let free to move. The results obtained from the free decay tests, measured by triaxial accelerometers, are shown in the following figure:

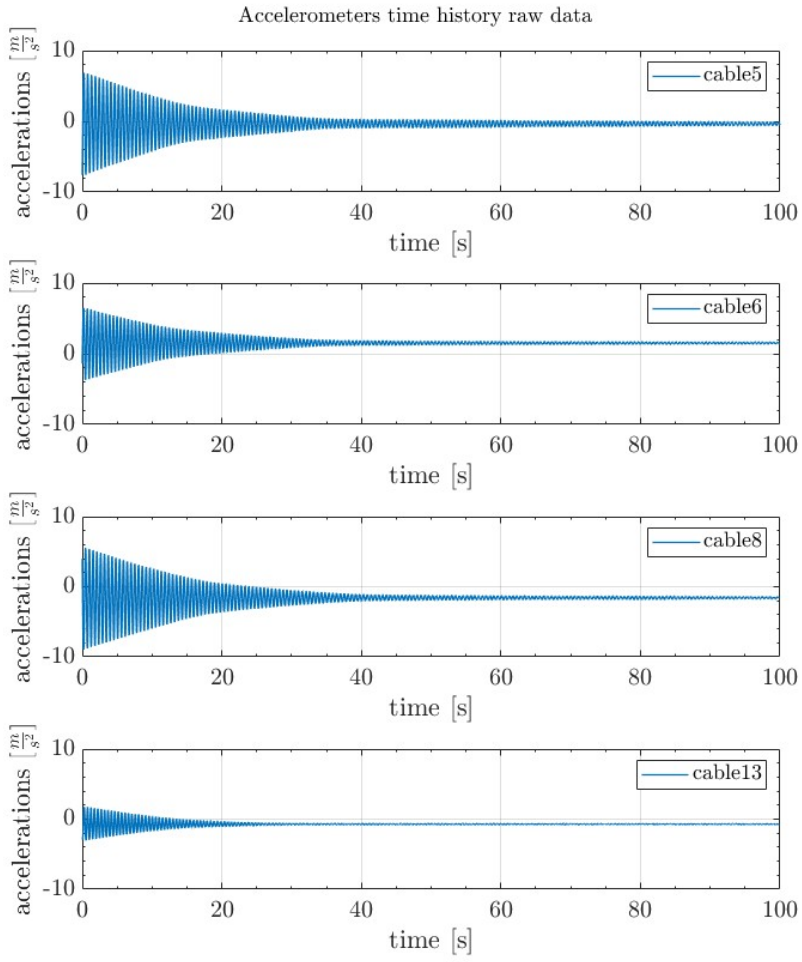

Figure 3: Hovenring bridge cable acceleration responses.

A decaying behaviour with decreasing amplitude is the trend expected. It can also be noticed that not all the signals are centered on the $y = 0$ coordinate axis, therefore the mean values is subtracted to each signal in order to allow proper data elaboration.
Beside that, in the decay plots 3 unexpected different regions are identified:

1. Large amplitude regions where it is found an higher slope and non linear effects dominating. As a matter of fact, the displacement field over the first cycles is no more compatible with the small displacement hypothesis.

The higher displacements the cable is subjected to, give rise to an increased final length of the cable, thus resulting in an increased tension. Since we are going to estimate the tension force as final goal, we cannot accept large displacement behaviour that are out of the usual system working conditions;

2. Decreased rate of decay with smaller amplitudes and smaller damping ratio;
3. Even smaller decay highlighting a region where the TMD is not working. Therefore this is not representative of the behaviour of the FE model, which is instead embedding also the information related to the TMD.

In light of this, the central region is the one that will be considered for the present analysis. From the free decay, h_1 and f_1 are estimated in the following sections.

3. Identification of the damping ratio

The computation of the non dimensional damping relies on the logarithmic decrement δ_i shown below:

$$\delta_i = \frac{1}{N} \log \left(\frac{\ddot{y}\left(t_i\right)}{\ddot{y}(t_{i+N})} \right) \tag{1}$$

where $\ddot{y}\left(t\right)$ is the acceleration at the instant t, N the number of peaks taken into account and T_i the period of oscillations. From the logarithmic decrement, the non dimensional damping ratio h_i has been derived:

$$h_i = \frac{\delta_i}{2\pi} \tag{2}$$

In green is highlighted the central portion of the acceleration data taken into account as stated in the previous section.

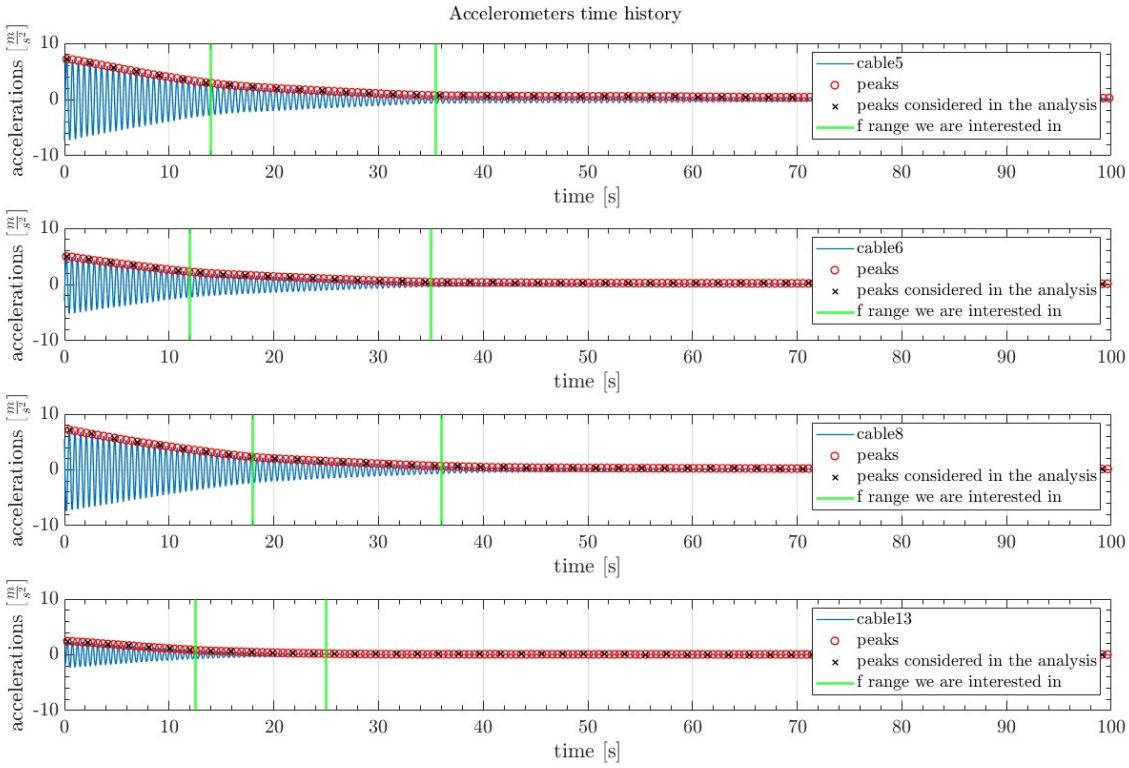

Figure 4: Free decay time history.

The logarithmic decrement is computed considering that for a damped system the envelope fits a negative exponential function and to obtain more accurate results one peak every four has been considered

for the analysis of both non dimensional damping and natural frequency ($N = 4$). Instead, the use of just subsequent peaks would have produced a measure more affected by noise.

The non dimensional damping ratio is thus calculated and its trend is shown in the following figure:

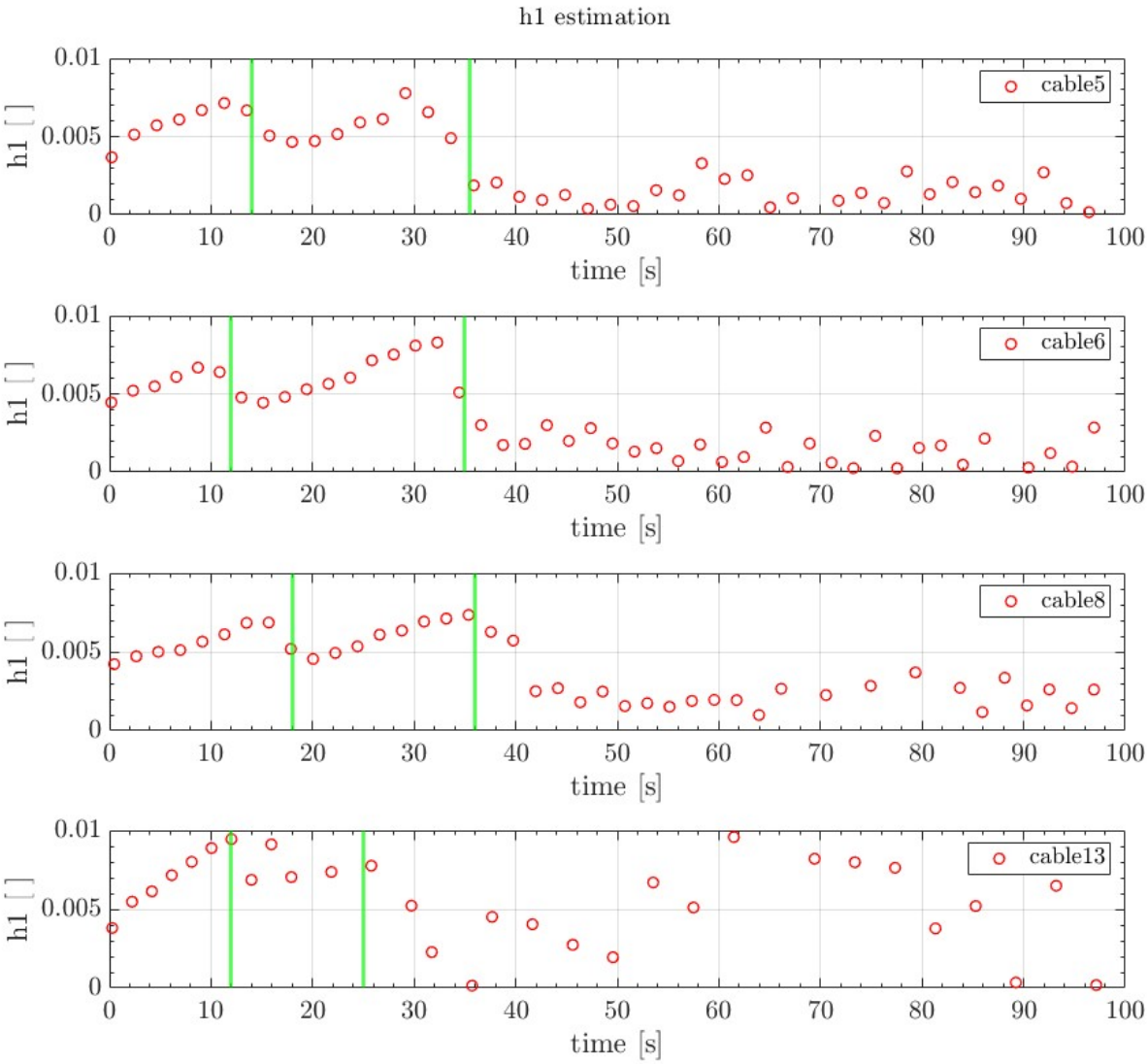

Figure 5: Non-dimensional damping ratio trend in time.

From Figure 5, over the first cycles of the data is seems that the non dimensional damping values increase. It is important to notice that this is not physically happening, it is just due to a decrease of the tension force that the system wants to apply in that region: it is not the damping that is increasing but it is the tension T that is changing. Thus, being the system trying to decrease the T produced by the large amplitudes of the response, the decrease is more than exponential, resulting in an increasing trend and not in a plateau for the h1 values.

As a general comment, due to the sampling of the data acquired ($f_s = 128Hz$), within each region a certain variability of the parameters we want to estimate is present: this is an effect due to the frequency resolution.

In order to get a smoother shape of the trend, a moving average filter is applied to the non dimensional

damping ratio results (Figure 6) and then the average among the values in the green region is performed for each cable (Table 1).

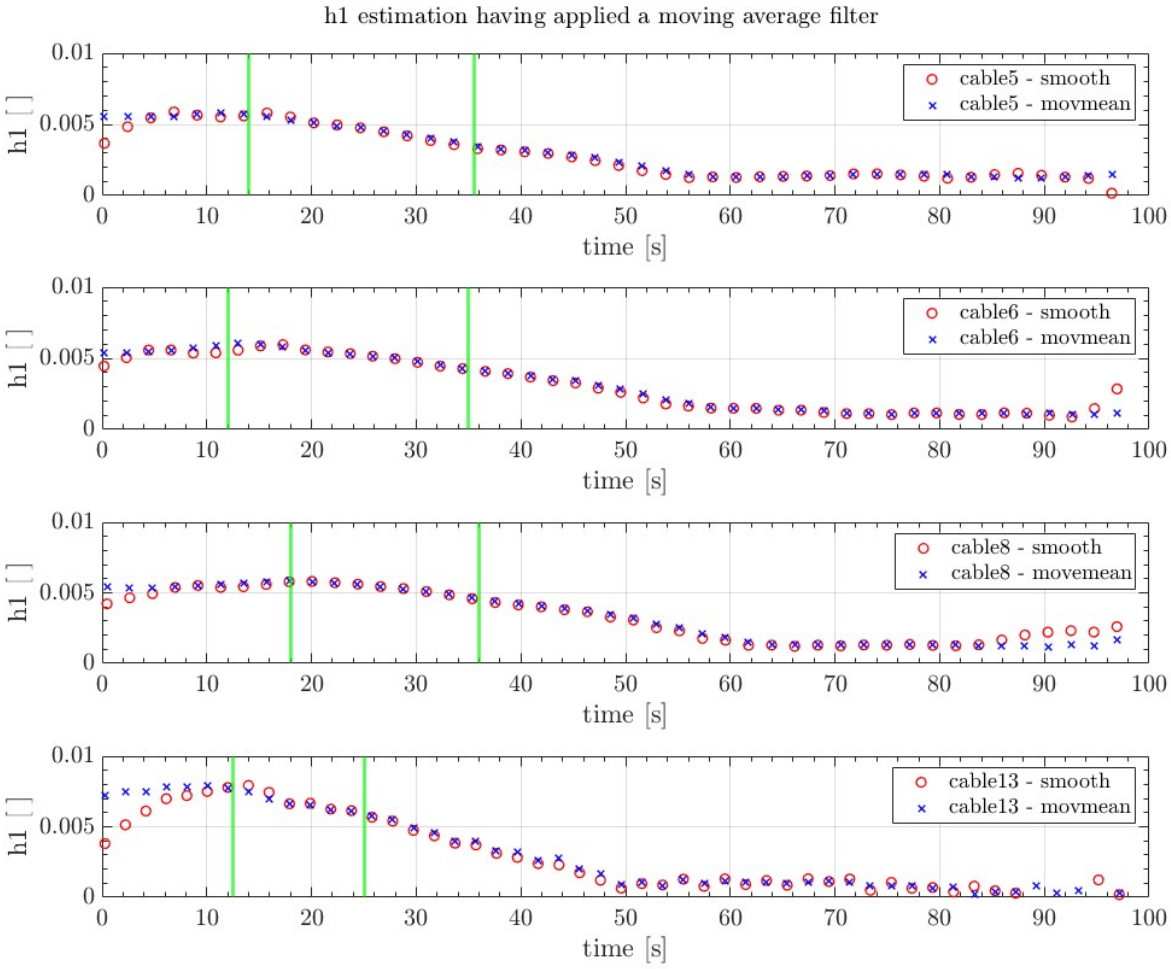

Figure 6: Non-dimensional damping ratio trend in time having applied 2 types of moving average filter.

In this last computation, two Matlab functions have been used to smooth the plot shape: *Smooth* and *Movemean*. As can be noticed from the graphs (Figure 6) and in the table below (Table 1) the differences between the results obtained from the 2 methods are negligible. The mean value of the h_1 values in the green region are shown below:

	cable5	**cable6**	**cable8**	**cable13**
$h1_{smooth}$[‰]	4.6960	5.2131	5.3013	6.8435
$h1_{movmean}$[‰]	4.6908	5.2692	5.3079	6.6560
$\Delta h1$[%]	0.11	1.08	0.12	2.74
$h1_{average}$[‰]	4.6934	5.2411	5.3046	6.7498

Table 1: Experimental non dimensional damping ratio assessment.

An average between the values obtained thanks to the 2 methodologies can be computed and considered as final h_1 result.

4. Identification of the first natural frequency

In order to find the first natural frequency, the oscillation period has been calculated, taking into account that in the free decay signals we have considered 1 peak every four to better deal with the noise associated to the measures.

$$T_i = \frac{(t_{i+N} - t_i)}{N} \tag{3}$$

$$f1_i = \frac{1}{T_i} \tag{4}$$

As previously mentioned, since the FE model is able to reproduce the system behaviour assuming both constant tension force and dampers' behaviour in their operative condition, only the linear region of the free decay data, interposed by the 2 green sectors, has been considered.

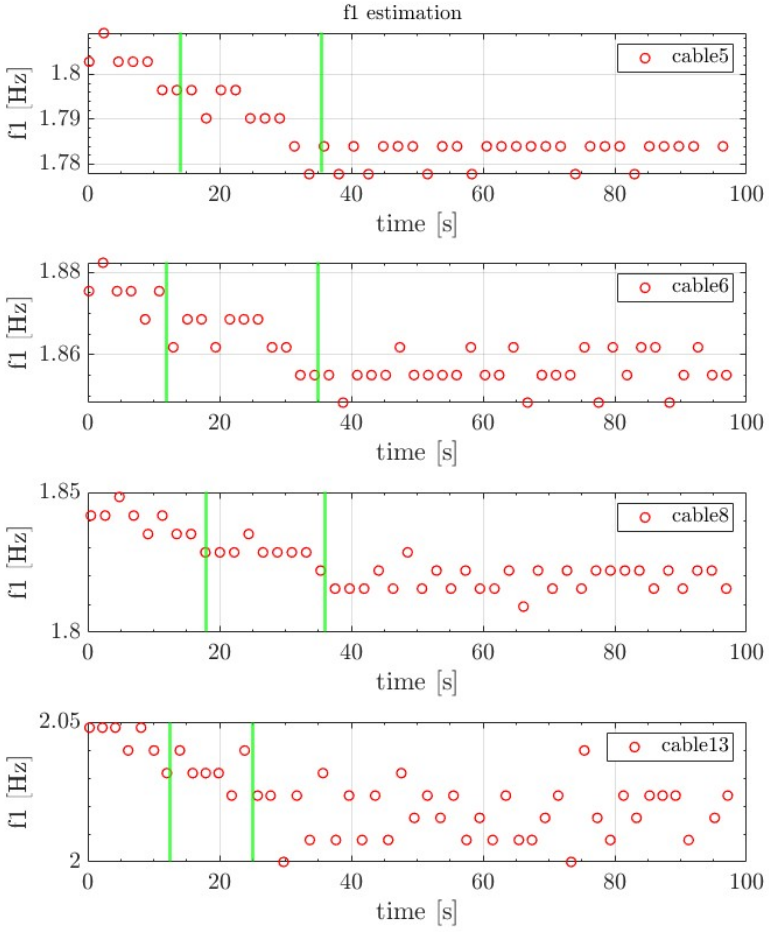

Figure 7: First natural frequency over time

There is a systematic behaviour of the cable that shows different f_1 at the beginning and at the end because of non-linearities: in the first region we have higher f_1 values due to the increased tension force provided by large displacements and deformations. Instead, in the third region values are smaller since the TMD are not effective. This also means that the length reached by the cable in the 2 zones (first and third) are different and, being the distance from the top to the bottom of the structure the same, the longer cable has higher tension T and higher f_1. Furthermore, as previously mentioned, the

f_1 variability is also due to the frequency resolution.

In the green region for all the cables the mean among the frequencies has been computed to finally get the first natural frequency as shown in the table below (Table 3).

	cable5	**cable6**	**cable8**	**cable13**
$f1_{experimental}$ **[Hz]**	1.7903	1.8337	1.8286	2.0331
$f1_{nominal}$ **[Hz]**	1.7635	2.0376	1.7343	2.0527
$\Delta f1$ **[%]**	1.5140	8.5346	5.4374	0.9549

Table 2: First natural frequency assessment.

5. FE model

The cables are modelled using an equivalent **tensioned beam** in the FE scheme, this because their bending stiffness properties are not negligible. As a matter of fact for each of them the following elements have been modelled from the deck to the pylon:

1. Threaded bar M100, used to constrain the cable to the deck side;
2. Socket, it realises the switching from the cable to the threaded bar;
3. Cable (full lock coil ⌀50 [mm]);
4. Socket;
5. Threaded bar M72, used to constrain the cable to the tower side;

All those mechanical components are different and, since the FE model is adopted to estimate in an indirect way the actual tension force in this structure, the model must be as accurate as possible.

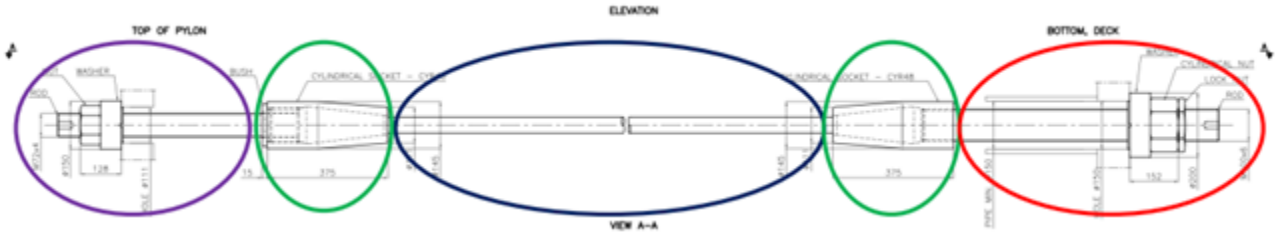

Figure 8: FE model of the physical system under analysis: the cable.

The mesh of the threaded bars and cables was carefully refined at the boundaries with the purpose of an optimum structure modelling at the locations of maximum bending.

As an example, in the following tables the mechanical properties for $Cable13$, found in the input file, are listed:

	m $[\frac{Kg}{m}]$	**EA [N]**	**EJ** $[Nm^2]$	**T [N]**
1	55.06	1.445E+09	8.06E+05	705e3
2	129.60	3.401E+09	4.47E+06	705e3
3	102.60	2.69E+09	2.80E+06	705e3
4	14.10	2.78E+08	2.75E+04	705e3
5	28.76	7.548E+08	2.20E+05	705e3

Table 3: Structure properties declared in the FE input file for $Cable13$.

The total number of elements used to discretise the structure is:

- 13 elements for the threaded bars;
- 12 for the sockets;
- 204 elements for the cable.

It is worth notice that in the Input file it is also embedded the information related to the variable amount of threaded bar that is fastened at the level of the deck or of the pylon.

Below, a picture of the undeformed structure model is shown: the deck side is depicted in upper position, while the pylon side is in the lower part.

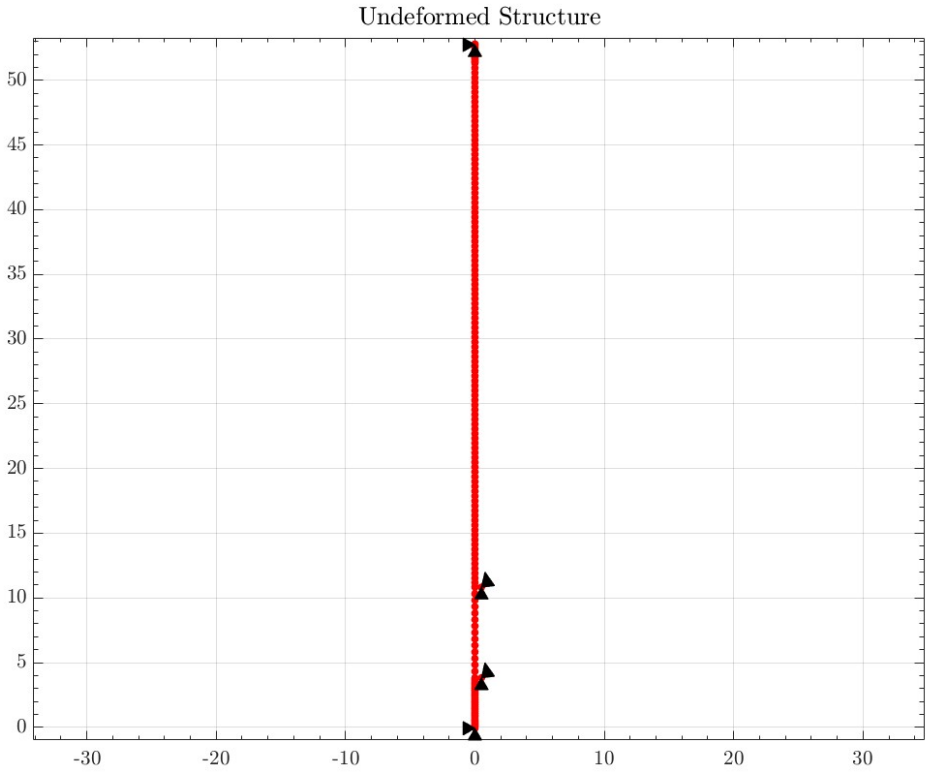

Figure 9: Undeformed configuration of *Cable*13 provided by the FE model.

As it can be noticed by the Input file below (Figure 12), there are 2 nodes constrained in x and y direction representing the initial and final pinned extremities of the structure. Then, 4 further nodes have been introduced in the modelization needed in order to take into account the TMDs presence.

```
! list of nodes :
*NODES
! n. of node - constraint code (x,y,theta) - x coordinate- y coordinate.
1       1       1       0       0       52.745
2       0       0       0       0       52.8
3       0       0       0       0       52.68333333
4       0       0       0       0       52.56666667
```

(a) First part of the nodes definition section

```
229     0       0       0       0       0
230     1       1       0       0       -0.068
231     0       1       1       0.5     10.827
232     0       1       1       0.5     10.827
233     0       1       1       0.5     3.827
234     0       1       1       0.5     3.827
! end card *NODES
*ENDNODES
```

(b) Last part of the nodes definition section

Figure 10: Input file *Cable*13.

The FE model considers 2 torsional springs in correspondence of the fist and last node, therefore one connected to the deck side and one on the pylon side (respectively: node 1 and node 230).

```
% Torsional spring - deck side
kT1 = 9e6;
i_ndof_spring = idb(1,3);
K(i_ndof_spring,i_ndof_spring) = K(i_ndof_spring,i_ndof_spring)+kT1;

% Torsional spring - tower side
kT2 = 9e6;
i_ndof_spring = idb(230,3);
K(i_ndof_spring,i_ndof_spring) = K(i_ndof_spring,i_ndof_spring)+kT2;
```

Figure 11: FE model torsional springs modelization (*Cable*13).

In fact, hinges and torsional lumped stiffness have been considered for a realistic model of the constraints. This choice is really important since the definition of the BCs affects the eigenfrequencies and mode shapes result; therefore the BCs have been chosen realising a best fitting of numerical and experimental modes for different types of BCs, just normalising the FE results thanks to the displacements obtained experimentally.
NB: this is done only for the first eigenfrequency.

Here instead, it is shown the modelization of the 2 TMDs placed on the pylon side. As a matter of fact, cables suffer from wind interaction (VORTEX INDUCED VIBRATIONS) experiencing large deformations that may lead to fatigue effects problematic for the bridge; thus, TMDs are needed.

```
% TMD 1 - 04R36 - Mass and stiffness
m_tmd1 = 4.93;
k_tmd1 = 2.12E+03;
i_ndof1 = idb(149,1);
i_ndof2 = idb(231,1);
i_dof_tmd1 = [i_ndof1 i_ndof2];

M(i_ndof2,i_ndof2) = M(i_ndof2,i_ndof2) + m_tmd1;

K_tmd1 = [k_tmd1 -k_tmd1; -k_tmd1 k_tmd1];
K(i_dof_tmd1,i_dof_tmd1) = K(i_dof_tmd1,i_dof_tmd1)+K_tmd1;

% TMD 2 - 04R36 - Mass and stiffness
m_tmd1 = 5.1;
k_tmd1 = 888;
i_ndof1 = idb(149,1);
i_ndof2 = idb(232,1);
i_dof_tmd1 = [i_ndof1 i_ndof2];

M(i_ndof2,i_ndof2) = M(i_ndof2,i_ndof2) + m_tmd1;

K_tmd1 = [k_tmd1 -k_tmd1; -k_tmd1 k_tmd1];
K(i_dof_tmd1,i_dof_tmd1) = K(i_dof_tmd1,i_dof_tmd1)+K_tmd1;
```

(a) TMD1 modelization (*Cable*13).

```
% TMD 1 - 4RZ11 - Mass and stiffness
m_tmd1 = 5;
k_tmd1 = 4.00E+03;
i_ndof1 = idb(164,1);
i_ndof2 = idb(233,1);
i_dof_tmd1 = [i_ndof1 i_ndof2];

M(i_ndof2,i_ndof2) = M(i_ndof2,i_ndof2) + m_tmd1;

K_tmd1 = [k_tmd1 -k_tmd1; -k_tmd1 k_tmd1];
K(i_dof_tmd1,i_dof_tmd1) = K(i_dof_tmd1,i_dof_tmd1)+K_tmd1;

% TMD 2 - 4RZ11 - Mass and stiffness
m_tmd1 = 7;
k_tmd1 = 1.17E+04;
i_ndof1 = idb(164,1);
i_ndof2 = idb(234,1);
i_dof_tmd1 = [i_ndof1 i_ndof2];

M(i_ndof2,i_ndof2) = M(i_ndof2,i_ndof2) + m_tmd1;

K_tmd1 = [k_tmd1 -k_tmd1; -k_tmd1 k_tmd1];
K(i_dof_tmd1,i_dof_tmd1) = K(i_dof_tmd1,i_dof_tmd1)+K_tmd1;
```

(b) TMD2 modelization (*Cable*13).

Figure 12: Input file.

Each damper is represented by **2 equivalent 1 DOF systems**. Also in this case, a good matching between the numerical model of the 2 equivalent systems and the manufacturer FRF has been derived, therefore the correct m1, k1, c1, m2, k2, c2 has been found.

Finally, the shape of the first mode of *Cable*13 is depicted below:

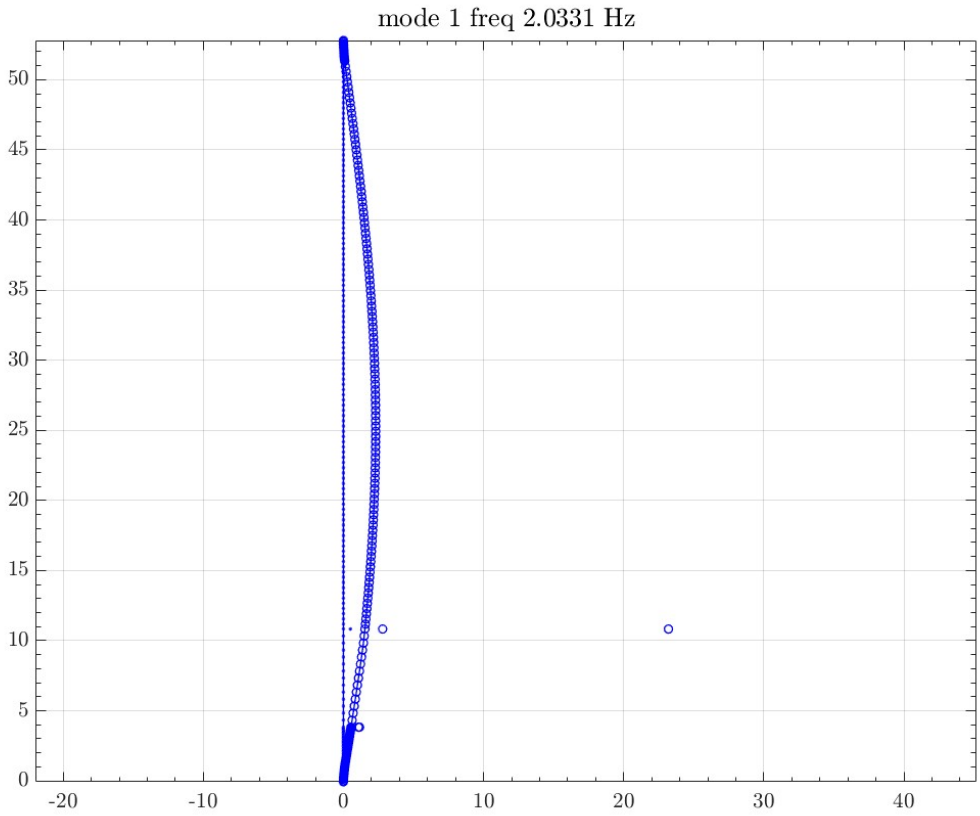

Figure 13: Mode 1 (*Cable*13).

It can be noticed that the 4 nodes constrained vertically and in the rotations have undergone an horizontal displacement coherent with their role: limiting transversal vibrations in correspondence of the natural frequency of the structure they want to protect and vibrating themselves.

6. Tension force estimation by the FE model and comparison nominal Vs actual tension values

The percentage variation between the nominal and numerical tension calculated by FE model is shown below:

	cable5	**cable6**	**cable8**	**cable13**
$T_{nominal}[kN]$	470	705	470	705
$T_{numerical}[kN]$	482.271	549.573	526.573	668.983
$\Delta T[\%]$	3.25	22.05	12.04	5.11

Table 4: Tension force comparison between nominal and numerical values.

The estimated tension is expected to be within the range $+/-5\%$ of the actual tension value, that is for us unknown. Moreover, provided that the estimation error for the tension force is twice the one for the frequency, the maximum error for the frequency estimation should be below 2%.

7. Hilbert transform: second way for modal parameters identification from decays

Envelope evaluation is an important signal processing technique, frequently used in damage identification and machinery monitoring, but herein used to characterize viscous structural damping. As a matter of fact, non dimensional damping parameter can be also computed with the Hilbert transform that is the convolution between a signal and $\frac{1}{\pi t}$. It can be considered as a filter shifting the phase of components of its input of $-\pi/2$ radians. The analytical signal is thus defined as:

$$AS(t) = x(t) + jy(t); \tag{5}$$

Using the Euler notation, the complex signal above can be expressed in terms of modulus and phase:

$$AS(t) = A(t)e^{-j\phi(t)}; \tag{6}$$

where A(t) is the envelope or amplitude of the analytic signal and ϕ(t) is the phase of the analytic signal.

The envelope signal can be used to identify the system damping, given that for a single DOF mechanical system the envelop signal should be exponential.

Once the envelope signal is known, it is possible to approximate the signal A(t) with an exponential curve as shown in the following figures (Figure 14, 15, 16, 17). Provided the regression curve, the non dimensional damping is calculated as:

$$h_i = \frac{\alpha}{\omega_{0i}} \tag{7}$$

where α is the exponent of the exponential regression.

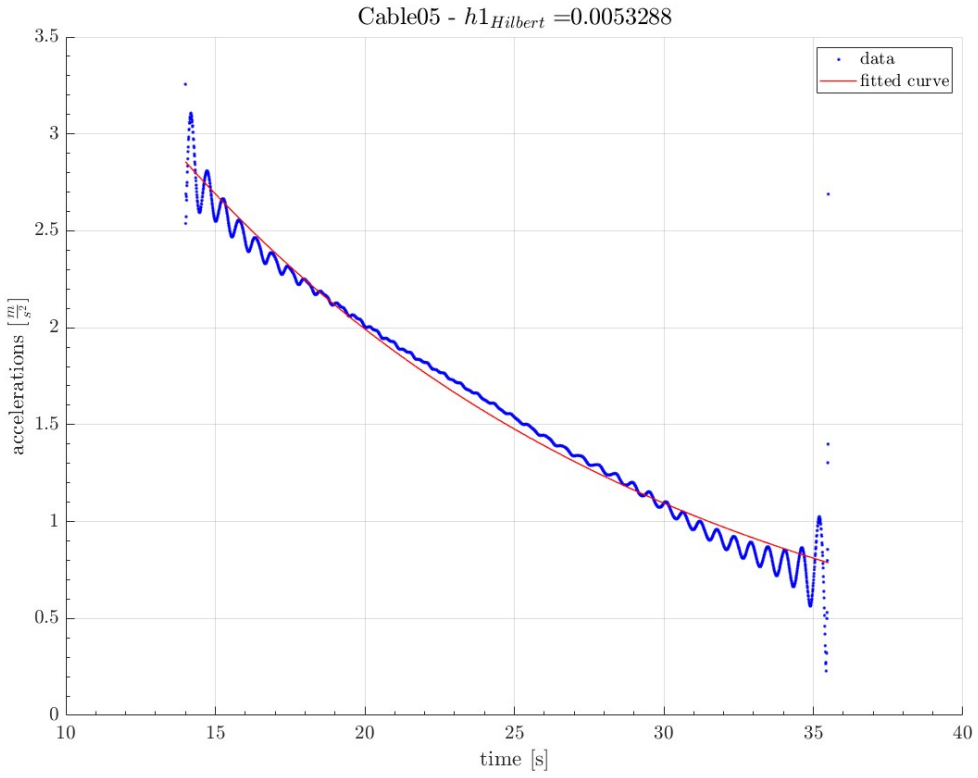

Figure 14: Hilbert assesment of non dimentional damping.

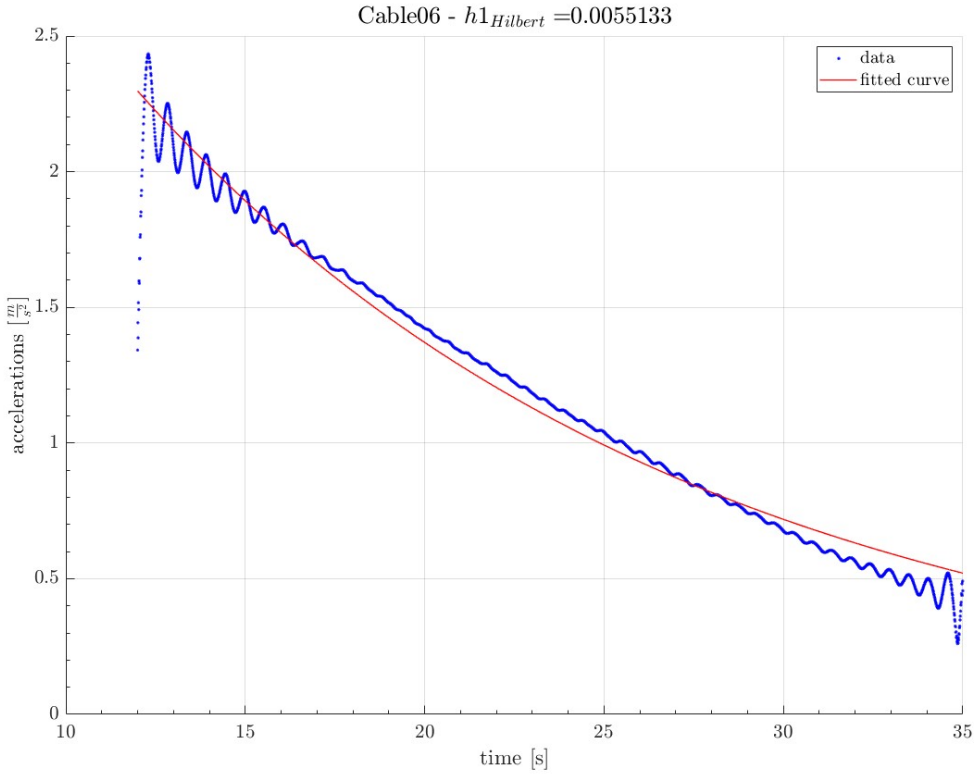

Figure 15: Hilbert assesment of non dimentional damping.

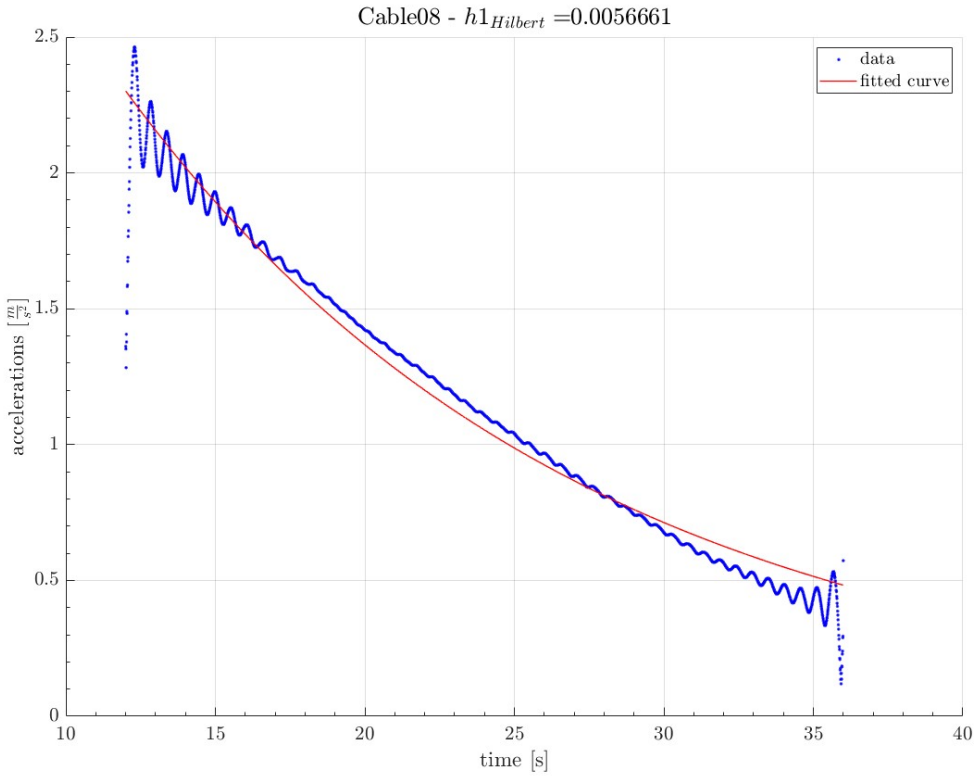

Figure 16: Hilbert assesment of non dimentional damping.

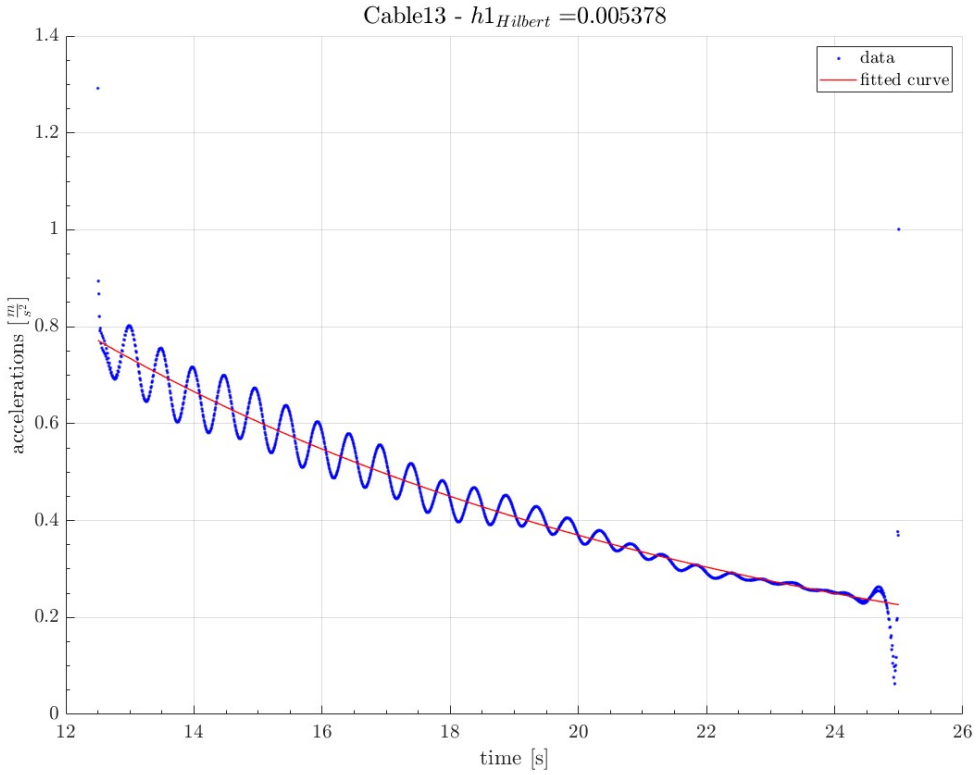

Figure 17: Hilbert assesment of non dimentional damping.

A direct comparison with the previous results obtained with the logarithmic decrement analysis is presented in the table below:

	cable5	**cable6**	**cable8**	**cable13**
$h1_{average-smooth-movemean}$[‰]	4.6934	5.2411	5.3046	6.7498
$h1_{Hilbert}$[‰]	5.3288	5.5133	5.6661	5.3780
$\Delta h1$[%]	13.53	5.19	6.81	20.32

Table 5: Experimental non dimensional damping ratio assessment (Hilbert).